Available online at www.sciencedirect.com

jmr&t Journal of Materials Research and Technology

journal homepage: www.elsevier.com/locate/jmrt

Original Article

Study on photoelectricity properties of SiCN thin films prepared by magnetron sputtering

Qiang Li [a,1], Cheng Chen [a,b,1], Mingge Wang [a], Yaohui Lv [a], Yulu Mao [a], Manzhang Xu [c], Yingnan Wang [a], Xuewen Wang [c], Zhiyong Zhang [a], Shouguo Wang [a], Wu Zhao [a,*], Johan Stiens [b,d]

[a] School of Information Science and Technology, Northwest University, Xi'an, 710127, PR China
[b] Vrije Universiteit Brussel (VUB), Dept. Electronics and Informatics (ETRO), Pleinlaan 2, Brussels, B-1050, Belgium
[c] Frontiers Science Center for Flexible Electronics, Xi'an Institute of Flexible Electronics (IFE) and Xi'an Institute of Biomedical Materials & Engineering, Northwestern Polytechnical University, Xi'an, 710129, PR China
[d] SSET Department, IMEC, Kapeldreef 75, Leuven, B-3001, Belgium

ARTICLE INFO

Article history:
Received 3 March 2021
Accepted 10 August 2021
Available online 13 August 2021

Keywords:
SiCN thin Films
Photoelectric properties
Magnetron sputtering

ABSTRACT

SiCN thin film is one of the most attractive silicon-based materials due to its excellent electrical, mechanical and optical properties. In this study, SiCN thin films have been prepared by the radio frequency reactive magnetron sputtering method under different sputtering power, pressure, and substrate temperature. The microstructure, morphology, and the optical and field emission properties of SiCN thin films were performed. The results indicated that the high-quality SiCN thin films have been successfully prepared and it is proved that these properties can be tailored by the preparation conditions. A main near ultraviolet light emission line at around 370 nm in SiCN thin films makes it suitable for the development of optoelectronic devices. This study can provide novel guidance for the controlled preparation of high-quality SiCN thin films by magnetron sputtering.

1. Introduction

As a typical ternary compound material, SiCN films show complex and uncertain microscopic structures, such as various cluster forms, multiple phase structures and bonding types, which are strongly dependent on elemental composition. SiCN films have excellent mechanical and optical properties, as well as field emission (FE) properties, which enables the films to be used in super-hard coatings, optical storage, LED devices and optoelectronic devices.

As is well known, the performance of the film device is mainly dependent on the quality of the films, which were largely affected by the preparation method, the raw material type and the treatment conditions [1–4]. It is possible to tailor these properties by adjusting the parameters of the deposition process. To obtain high-quality SiCN films, many approaches have been adopted. Kozak A. O. et al. prepared

* Corresponding author.
E-mail address: wzhao@nwu.edu.cn (W. Zhao).
[1] These authors contributed equally to this work.
https://doi.org/10.1016/j.jmrt.2021.08.043

SiCN films by using plasma-enhanced chemical vapor deposition (PECVD) at different nitrogen flow rates, and found intensities of the main peaks in fluorescence spectra increase with increasing nitrogen content at about 440 nm [5]. Swain B. P. et al. prepared SiCN thin films by hot wire chemical vapor deposition (HWCVD), and found carbon network bonding change from sp^2 to sp^3 due to the introduction of nitrogen [6]. Wrobel A. M. et al. synthesized SiCN films by using microwave plasma chemical vapor deposition (MPCVD) and investigated its microstructure and morphology, and the results indicate that the SiCN films could be used for optical and electronic devices [7]. All these literature prove that the CVD-based method is the most appropriate to prepare the SiCN thin films. However, the hydrogen impurity was introduced into the SiCN films inevitably by using these methods. At the same time, the systematic study of controlled preparation of SiCN thin films is also rarely reported. To prevent the introduction of impurity hydrogen, sputtering methods are a better option for the preparation of the SiCN films. Particularly, the radio frequency reactive magnetron sputtering is one of the candidates sputtering methods for the preparation of the SiCN thin films. In this study, the SiCN films were synthesized by radio frequency reactive magnetron sputtering method. The relationship between the composition, morphology, optical, FE properties, and the preparation parameters (including sputtering power, sputtering pressure and substrate temperature) have been systematically investigated. The results show that the preparation conditions have considerable influence on SiCN thin films on the microstructure, PL, and FE properties. Our present study will provide a reference for the future development of high-performance SiCN thin films.

2. Experimental

2.1. Materials and method

SiCN thin films were deposited by using radio frequency magnetron sputtering method. High purity raw silicon nitride target and graphite target with a diameter of 60 mm were customized as source of silicon, carbon, and nitrogen elements. Argon gas was purchased with purity of 99.999% as working gas. The Si/SiO_2 wafers and quartzes were purchased as substrates. The substrates were ultrasonically cleaned with acetone-tetrachloromethane solution, ethanol, and deionization to remove contaminants from the surfaces. Before sputtering, the targets were pre-sputtered for 30 min to remove surface oxide layer and absorbed. To investigate the influence of target powers on the structure and properties of the SiCN thin films, the target power of silicon nitride was set at 100 ~ 190 W and the graphite target power was 80 ~ 110 W. The distance between substrate and targets was fixed at 50 mm. Argon gas was continually introduced into the chamber with a flow rate of 30 sccm, and the gate valve of the chamber has been adjusted so that the pressure in the chamber was 7 Pa. The substrate holder was kept revolving during the sputtering to ensure uniform distribution of composition on the substrates. The SiCN thin films were deposited for 90 min at room temperature (RT). Details of deposition parameters are shown in Table 1. In addition, some other experiments then set up to investigate the influence of chamber pressure and substrate temperature on the thin films as shown in Table 1.

2.2. Characterization

The crystal structure of the SiCN films was obtained by using a SHIMADZU 6100 X-ray diffraction (XRD). The chemical bonding structure of the films was determined by a Nicolet Nexus 410 Fourier transform infrared spectroscopy spectrometer (FTIR) and a Kratos Analytical AXIS supra X-ray photoelectron spectrometer (XPS). The carbon phase in the films was analyzed by HORIBA Xplora plus Raman microscopy. Surface morphology and roughness of the films were obtained by a Carl Zeiss SIGMA scanning electron microscope (SEM) and an Asylum Research Cypher S atomic force microscope (AFM). The transmittance of the deposited films on the quartz substrates was measured by a SHIMADZU UV-3150 ultraviolet–visible (UV–Vis) spectrophotometer. The photoluminescence (PL) properties of the films were measured by HORIBA FluoroMax-4p fluorescence spectroscope. The field emission (FE) performance of the films was measured by an apparatus with a two-parallel-plate configuration in a vacuum chamber, and a constant voltage source was used to provide the dc voltage and an ammeter to monitor the current value during the test.

Table 1 – Preparation parameters of SiCN films. Label TP-7, SP-3 and ST-1 are the same work, which are presented three times for the convenience of data presentation.

entry	power of silicon nitride target (W)	power of graphite target (W)	sputtering pressure (Pa)	substrate temperature (°C)
TP-1	100	80	7	RT
TP-2	100	90	7	RT
TP-3	100	100	7	RT
TP-4	100	110	7	RT
TP-5	130	80	7	RT
TP-6	130	90	7	RT
TP-7	130	100	7	RT
TP-8	130	110	7	RT
TP-9	160	80	7	RT
TP-10	160	90	7	RT
TP-11	160	100	7	RT
TP-12	160	110	7	RT
TP-13	190	80	7	RT
TP-14	190	90	7	RT
TP-15	190	100	7	RT
TP-16	190	110	7	RT
SP-1	130	100	3	RT
SP-2	130	100	5	RT
SP-3	130	100	7	RT
SP-4	130	100	9	RT
ST-1	130	100	7	RT
ST-2	130	100	7	500
ST-3	130	100	7	600
ST-4	130	100	7	700

3. Results and discussions

3.1. *Structure, chemical bonding configurations and compositions of SiCN thin films*

For studying the microstructure of as-deposited SiCN thin films, the XRD spectra were tested. Fig. 1(a–d) represent the XRD patterns of the samples which sputtered with silicon nitride target power ranged from 100 to 190 W, respectively. The diffraction peaks located at about 38.1°, 44.4°, 64.8°, and 77.9° belonged to the nanocrystalline phase of SiC (JCPDS No. 49-1623). A segment of the spectra with 2θ from 53° to 60° were truncated, as the presence of an intense diffraction peak centered at approximately 54.2° makes other pivotal peaks unreadable. This peak could be corresponding to the SiO_2 phase, which may be caused by the oxidation layer on the surface. As seen from these graphs, the intensities of the peaks increased at first and then decreased with the silicon nitride target power increasing from 100 to 190 W. Similarly, when the power of graphite target was changed, the intensity of diffraction peaks had the same tendency. It was found that the intensity of sample TP-7 was stronger than others, which was deposited by the sputtering of silicon nitride and graphite target with the power of 130 and 100 W, respectively. That means, unbefitting sputtering power will be averse to the formation of nanocrystals. The film would have the best crystallinity when the sputtering power of silicon nitride and graphite target is 130 and 100 W, respectively. Compared with the XRD standard card, it is found that all the peaks were shifted to higher angles. It is mainly caused by the entry of N atoms into the SiC nanocrystal and replacing C atoms to form N-doped SiC nanocrystals. The covalent radius of C atom is 0.077 nm, and the value of N atom is 0.075. Hence, the lattice constant of SiC nanocrystal decreased due to the substitution of N atoms for C atoms, which leads to the shifting [8]. Fig. 1(e and f) exhibits the XRD patterns of the as-deposited thin films prepared with different sputtering pressures and substrate temperatures. It shows that the intensity of the SP-1 diffraction peaks is strongest among the films prepared with different sputtering pressures, and the peak intensity diminished gradually with the pressure increased from 3 to 9 Pa. It indicates that films with better crystallinity can be obtained at low sputtering pressure (3 Pa). When the pressure is high, there are more argon molecules in the chamber, and the target atoms are more likely to collide with argon molecules in the process of moving from the targets to the substrate. It reduces the kinetic energy of the detached target atoms, which is not conducive to the formation of bonds and leads to poor crystallinity. The XRD spectra of the films prepared with different substrate temperatures shows that the strongest peaks appear in ST-2, and the peaks reduce distinctly when the substrate temperature increases or decreases. When the substrate temperature increases from room temperature to 500 °C, the crystallinity of the films becomes obviously better. But with the increase of temperature (up to 700 °C), the crystallinity becomes gradually worse. When the temperature rises to 500 °C, the crystallinity of the film becomes better, because the increase of temperature is conducive to crystallization. But as temperatures rise, nitrogen is more likely to replace carbon to form a chemical bond with silicon, making the Si–C bond less [9].

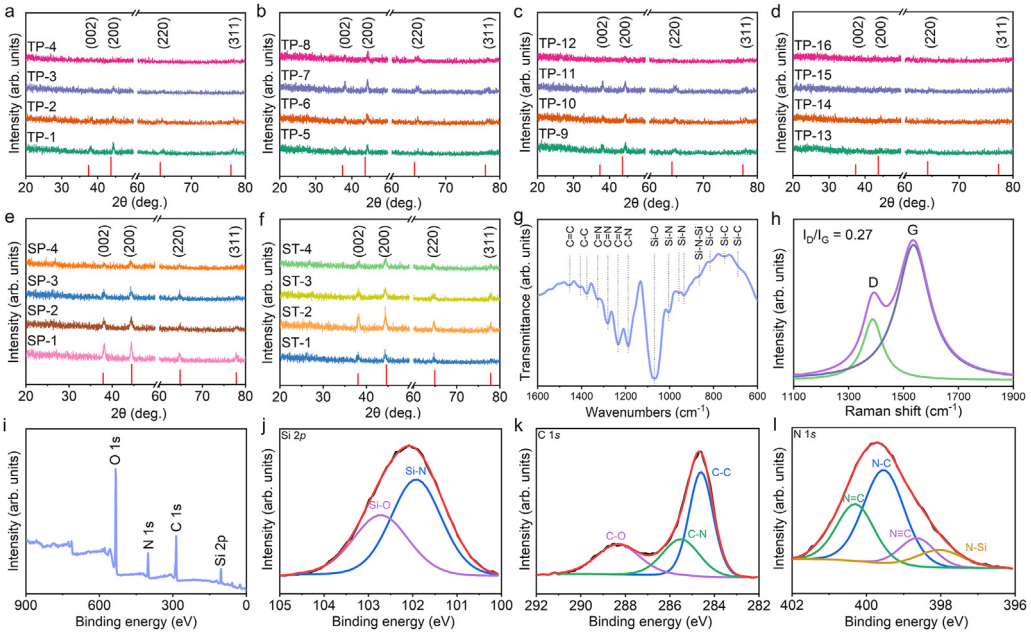

Fig. 1 – XRD patterns with target powers of silicon nitride are (a) 100, (b) 130, (c) 160 and (d) 190 W respectively, and graphite target power ranging from 80 to 110 W. XRD patterns of the films with (e) different sputtering pressures and (f) different substrate temperatures. The red vertical bars above the horizontal axes are the corresponding peak of the JCPDS card No. 49-1623. (g) FTIR and (h) Raman spectra of SiCN thin film deposited with silicon nitride sputtering power of 130 W and graphite sputtering power of 100 W (sample TP-7). XPS spectra: (i) elemental survey, (j) Si 2p, (k) C 1s, (l) N 1s for sample TP-7.

FTIR and XPS techniques are often used to verify the bonding structure, while Raman is often used to confirm the presence of carbon in the material. We have tested the bonding structure of SiCN thin films with Fourier transform infrared spectroscopy spectrometer, X-ray photoelectron spectrometer and Raman microscopy. The spectra of TP-7 were shown in Fig. 1(g-l) as obtained in the previous study [10]. The results show that the structures of the prepared thin films are ternary systems, each element in the ternary system was combined with the other two elements to form a complex network with bonds of Si–C, Si–N, Si–C, C–C, C–N, C–O, N–Si, N≡C, N–C and N=C.

3.2. *Morphologies of SiCN thin film*

Fig. 2(a) exhibits the surface SEM image of the sample TP-7 as typical. The cross-sectional images (Fig. 2(b)) show that homogeneous films were deposited on the substrates. The thicknesses of the samples prepared by different graphite sputtering powers (TP-5, TP-6, TP-7) are all about 120 nm except for TP-8 (138 nm). The thickness increases gradually from 111 to 159 nm as the sputtering power of silicon nitride target increases from 100 W to 190 W. The deposition rate can provide reference for preparing SiCN films with required thickness. The deposition rates were determined to be 1.33–1.53 nm/min by calculating the ratio of thicknesses to sputtering time as the graphite sputtering power ranged from 80 to 110 W. Similarly, the deposition rates of TP-3, TP-7, TP-11 and TP-15 were calculated to be 1.23, 1.33, 1.52 and 1.76 nm/min, respectively. The results indicate that higher sputtering power within a reasonable range can accelerate the deposition. This is because the energy of argon ions is causally related to sputtering power. Higher sputtering power will increase the energy of argon ions, so that more atoms of the targets can be bombarded away from the targets, resulting in an increase in the thickness of the deposited film. The image of TP-7 was repeatedly placed for intuitively comparing the effects of different preparation conditions on the film thickness.

The surface morphology of TP-7 was also investigated by AFM. 2D and 3D AFM images with transverse dimension of 3.5 μm × 3.5 μm (Fig. 2(c and d)) show that the film surface is composed of spiculate structure. These images were processed and analyzed by software Igor Pro 6.37. The average height of the spiculate structures above the surface as shown in Fig. 2(e) is about 4.5 nm from the cross-sectional analysis at the line position in Fig. 3(c). As the most widely used parameter for characterizing film surface roughness, the root-mean-square roughness (RMS) of TP-7 was also calculated to be 2.2 nm. These values are small in relation to the thickness of the film, indicating that the surface of as-prepared SiCN is flat.

3.3. *Photoelectric properties of SiCN thin films*

Fig. 3(a) exhibits the optical transmission spectra of SiCN thin films deposited on quartz substrates which are labeled

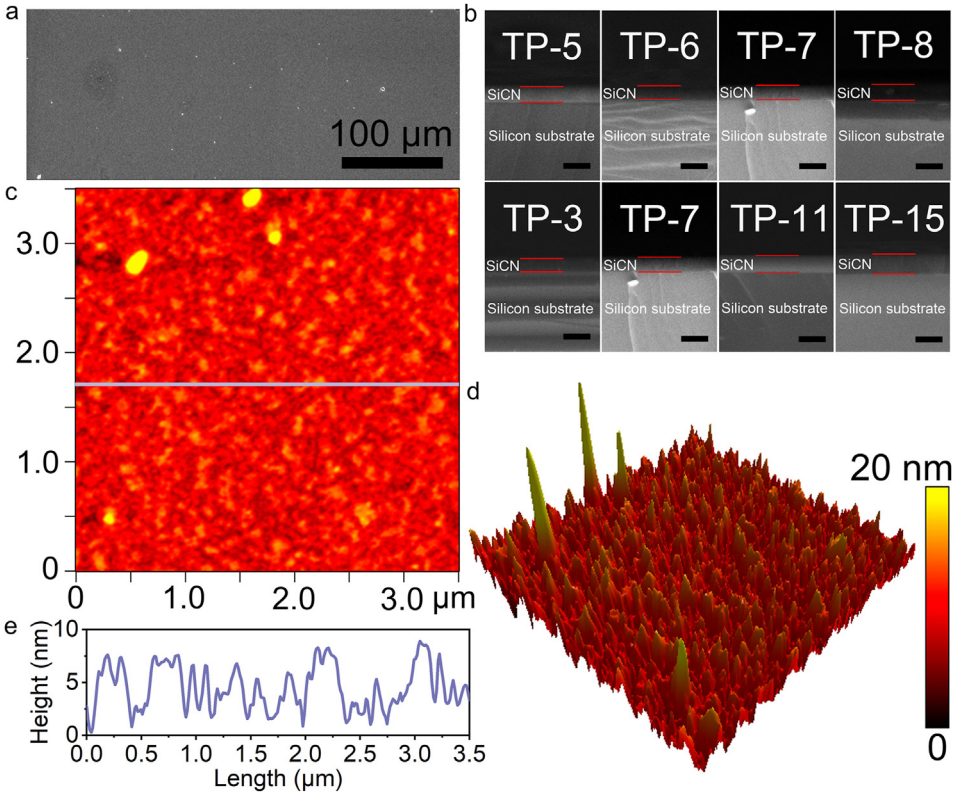

Fig. 2 – Morphology characterization of SiCN thin film. (a) Vertical view of SEM image of sample TP-7. (b) Cross-sectional SEM images, the boundaries of SiCN thin films are marked with two red lines in each graph with the silicon substrate below, scale bars: 200 nm. (c) 2D and (d) 3D AFM image of sample TP-7. (e) Cross-sectional image analysis of TP-7.

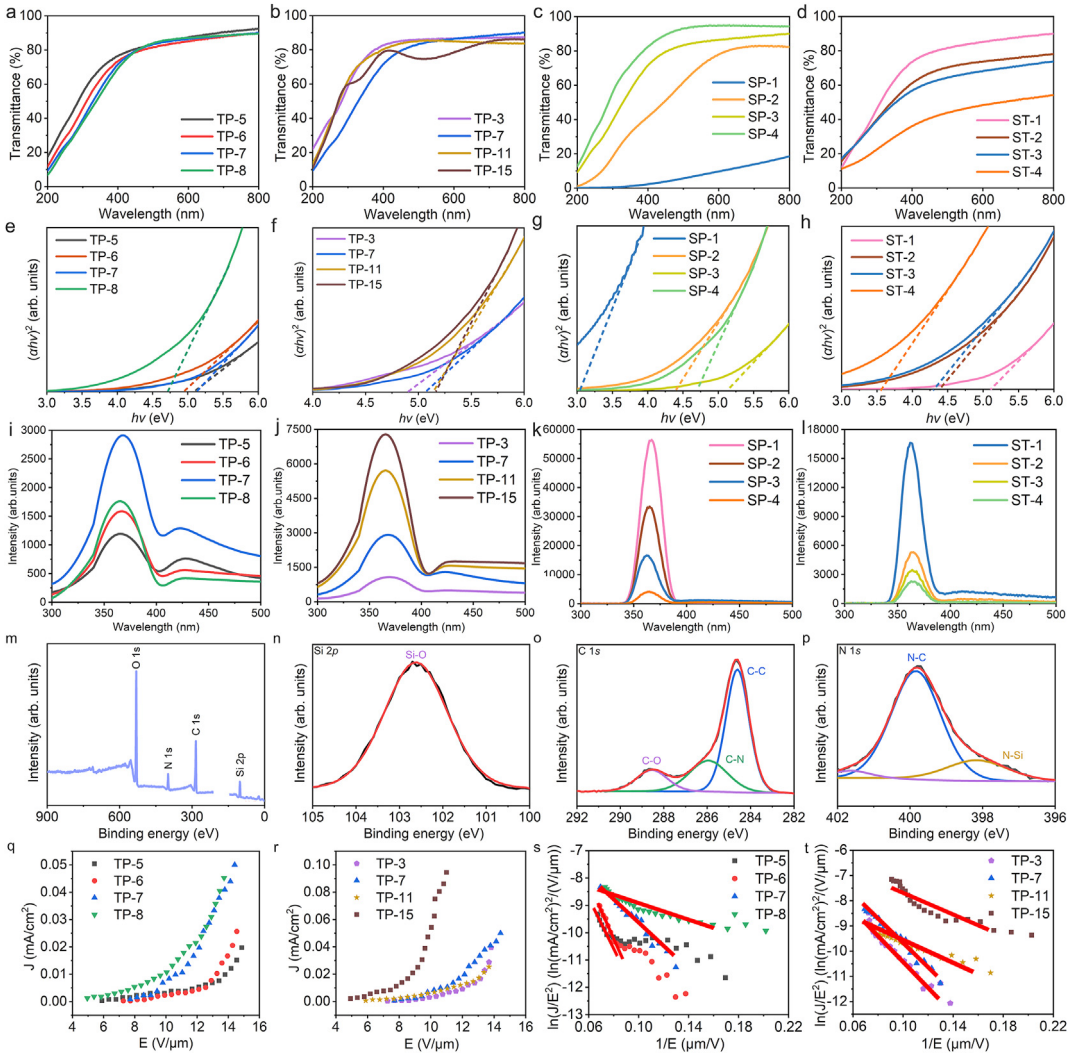

Fig. 3 – Transmittance of samples deposited with (a) silicon nitride target power was 130 W, (b) graphite target power was 100 W, (c) different sputtering pressures and (d) different substrate temperatures. (e–h) Tauc plots versus photon energy with linear fits (dash lines) for (a–d). (i–l) PL spectra of the SiCN thin films for (a–d). XPS spectra: (m) elemental survey, (n) Si 2p, (o) C 1s, (p) N 1s for sample TP-15. J-E curves of samples deposited with (q) silicon nitride target power was 130 W, (r) graphite target power was 100 W. The Fowler-Nordheim (F–N) plots of SiCN thin films prepared with (s) different sputtering pressures and (t) different substrate temperatures.

TP-5, TP-6, TP-7 and TP-8 with different graphite target power, and absorption spectra of sample TP-3, TP-7, TP-11 and TP-15 with different graphite target power are shown in Fig. 3(b). The transmittances of SiCN thin films deposited on quartz plate substrates increase rapidly with the wavelength from 200 to 400 nm and perform a transmittance over 70% in the visible region, indicating that these films have potential applications as highly transparent coatings in optical devices. The optical band gap of SiCN thin films could be effectively studied by optical absorption spectral analysis. This is because some basic electronic properties of the crystal state, such as the allowed bands and the energy gap, can be preserved due to the existence of the short-range ordered in the film [11].

Optical band gaps of the SiCN thin films can be estimated based on the Tauc equation as,

$$(\alpha h\nu)^2 = A(h\nu - E_g)$$

where $\alpha = -\ln(T\%)/d$ is the absorption coefficient, $h\nu$, A, Eg, T and d are the photon energy, constant, optical band gap, transmittance and thickness, respectively. $(\alpha h\nu)^2$ versus $h\nu$ in coordinate system was plotted as shown in Fig. 3(e and f). Optical band gaps of the samples can be determined by the linear fits of the curves' straight part. It can be known from the intersections of linear fits and horizontal axis that the optical band gap is between 4.7 and 5.1 eV. Besides, the optical band gap of SiCN thin films tend to increase as the graphite sputtering power increases, and an opposing tendency appears with an increasing sputtering power of silicon nitride. This is considered to be caused by the formation of Si_3N_4 and SiC, which has a band gap of 5.0 and 2.86 eV,

respectively. From the results, it can be deduced that the ratio of SiC/Si_3N_4 in the as-deposited SiCN films increases with an increasing sputtering power of the graphite/silicon nitride target, respectively. So, the optical band gap changes. Fig. 3(c and d) shows the optical transmittance of SiCN films prepared at different sputtering pressures and substrate temperatures. Both factors have a great influence on the transmittance of the film. The transmittance increases significantly with the sputtering pressure increasing from 3 to 9 Pa, whereas the value gradually decreases with the temperature increasing from room temperature to 700 °C. The optical band gap varies in a wide range due to their large differences in transmittance as shown in Fig. 3(g and h). The optical band gap increases from 3.0 to 5.1 eV as the pressure increases and decreases from 5.1 to 3.6 eV as the temperature increases from room temperature to 700 °C. Similarly, the difference in pressure and temperature leads to the different values of SiC/Si_3N_4. This result is consistent with XRD.

The PL spectra of SiCN thin films were also measured at room temperature with an excitation wavelength of 325 nm. Fig. 3(i) shows the PL spectra of the sample TP-5, TP-6, TP-7 and TP-8; and Fig. 3(j) displays the spectra of samples TP-3, TP-7, TP-11 and TP-15. Two PL peaks at around 370 and 425 nm can be seen in all the spectra. The PL peak at 370 nm in near ultraviolet region can be considered as the existence of an emission center, which may be caused by intrinsic defects in SiO_x ($x < 2$) [12,13]. While, the peak located at 425 nm was attributed to the SiC crystallite [12]. The result shows that the intensity of PL peaks increases with the sputtering power of graphite target enhancing from 80 to 100 W. However, the intensity decreases as the power continues increasing to 110 W. As the sputtering power of silicon nitride target increases from 100 to 190 W, the intensity of the PL peak located at 370 nm kept growing. The high sputtering power leads to insufficient bonding between atoms, resulting in an increase in the number of dangling bonds. Therefore, when the thin films were placed in air, more oxygen molecules would be attached to the dangling bonds. PL spectra in Fig. 3(k and l) show that the PL intensities of the SiCN films decrease by 14 and 7.5 times when the sputtering pressure increased from 1 to 9 Pa and temperature raised from RT to 700 °C, respectively. Hence, for better PL performance, lower pressure and/or temperature should be used in sputtering.

Considering that the sample has insensitive PL yield (TP-15) which is prepared with high sputtering power of silicon nitride target (190 W), the XPS spectra of the sample TP-15 was measured as shown in Fig. 3(m-p). For comparison, binding energy and intensity ratio of both sample TP-7 and TP-15 for each related chemical binding states are listed in Table 2. The Si 2p peak of the TP-15 was deconvoluted into a peak centered at about 102.6 eV as shown in Fig. 3(n), which is corresponded to Si–O bonds. The peak of C 1s can be assigned to peaks at 284.6, 286.0 and 288.5 eV as shown in Fig. 3(o), which are attributed to C–O, C–C and C–N bonds, respectively. The N 1s was deconvoluted into peaks centered at about 398, 399.8 and 401.6 as shown in Fig. 3(p), which are attributed to N–Si, N–C and N=C bonds, respectively.

The relative concentrations of the bonds in sample TP-7 and TP-15 are listed in the last two columns of Table 2. The results showed that the concentration of Si–O bond in TP-15 was much higher than that in TP-7 (about 2.5 times). The energy of Ar^+ increased as the sputtering power of silicon nitride target increased, so that more particles were detached from the target and more Si dangling bonds were formed on the film surface. The oxygen in the air will be absorbed to the surface of the film when the film is exposed to the ambient atmosphere.

The AFM image in Fig. 2(d) shows that many microtips appeared on the surface of the as-prepared SiCN thin film. Therefore, the FE performance of SiCN thin film is worth studying. Fig. 3(q and r) shows the emission current density (J) as a function of applied field (E) of partial SiCN thin films. The curves of films bring out exponential functions. The J-E curves of all samples are relatively smooth and consistent, indicating that SiCN thin films exhibit good stability in FE. The turn-on field indicates the level of an electron to be emitted from a material by an external electric field and it was defined as the value of E when J is 10 μA/cm^2. According to the J-E curves in Fig. 3(q), the turn-on fields of samples TP-5, TP-6, TP-7 and TP-8 are 13.83, 13.21, 11.24 and 9.80 V/μm, respectively. The turn-on fields of TP-3, TP-7, TP-11 and TP-15 are decreased from 12.09 to 7.67 V/μm as the silicon nitride target power increases from 100 to 190 W (Fig. 3(r)). Obviously, the turn-on fields of the SiCN thin films shrink with the sputtering power of graphite or silicon nitride target increasing. The maximum emission current density J_{max} of samples TP-5, TP-6, TP-7 and TP-8 are 19.7, 25.6, 50.0 and 45.2 μA/cm^2. While the J_{max} of samples TP-3, TP-7, TP-11 and TP-15 are 39.4, 50.0, 45.8, 94.4 μA/cm^2, respectively. The J_{max} of SiCN thin films tends to increase as the sputtering power of graphite or silicon nitride targets increasing. The minimum turn-on field is 7.67 V/μm and maximum emission current density J_{max} is 94.4 μA/cm^2 when the sputtering power of silicon nitride and graphite

Table 2 – Binding energy and intensity ratio for each related chemical binding state [14–18].

Element line	Chemical bond	Binding energy (eV)	Relative intensity (%) In sample TP-7	Relative intensity (%) In sample TP-15
Si 2p	Si–N	101.9	9.27	0
	Si–O	102.6, 102.7	6.77	16.85
C 1s	C–C	284.6	28.71	39.30
	C–N	285.5, 286.0	14.78	16.34
	C–O	288.3, 288.5	15.12	9.16
N 1s	N–Si	398.0	2.61	3.50
	N≡C	398.6	3.26	0
	N–C	399.5, 399.8	12.54	14.09
	N=C	400.3, 401.6	6.94	0.76

target is 190 and 110 W, respectively. In conclusion, a higher target power can improve the FE performance of SiCN thin films. Although the FE performance of as-prepared SiCN thin films is weak, the surface morphology with dense tips can be obtained by changing the preparation method and/or preparation conditions to enhance the performance. To better study the FE property of SiCN thin film, the Fowler-Nordheim (F–N) curves were rendered by plotting $\ln(J/E^2)$ versus $1/E$ to show the characteristics of I–V (Fig. 3(s and t)). The ratio of the local electric field of microtips to the applied electric field is defined as the field emission enhancement factor. This factor represents the degree of field emission enhancement on the surface of the SiCN thin film, which can be obtained by calculating the slope of the F–N curves. According to the F–N formula (as follows), the slope of the linear part of the plot is proportional to $-\phi^{\frac{3}{2}}/\beta$. That is, β is inversely related to the absolute slope.

$$J=\frac{A(\beta E)^2}{\phi}\exp\left(-\frac{B\phi^{3/2}}{\beta E}\right)$$

where A and B are constants, β is field enhancement factor, E is applied electric field, ϕ is work function of the material. Since the work function of the prepared SiCN thin film has not been determined, the value of β cannot be calculated. However, we could derive the trend of β caused by the change of preparation conditions from F–N plots. In general, the absolute value of the slope of F–N plot decreases as the sputtering power of the target increases. Therefore, the field enhancement factor β shows an increasing trend.

4. Conclusions

The high-quality SiCN thin films were successfully deposited on the silicon and quartz substrates by radio frequency reactive magnetron sputtering method with the graphite and silicon nitride target in an argon atmosphere. We found that the structure and photoelectric properties of the films can be controlled by tailoring the target power, sputtering pressure and substrate temperature. The effectiveness of different sputtering power, sputtering pressure and substrate temperature on prepared thin films have been investigated. The results show that the films are composed of elements Si, C and N, which formed chemical bonds in pairs. The thicknesses of as-deposited films are in the range of 111~159 nm. Sputtering power has little effect on the transmittance of the films, and it performs over 70% in the visible region. From the comparison, the higher sputtering power, lower pressure, or lower substrate temperature can make the PL performance of SiCN thin film better. The FE performance of the film becomes better with the increasing sputtering power of either silicon nitride or graphite target. Blue-violet light emitting properties of the SiCN thin films make them suitable for application in optoelectronic devices.

Declaration of Competing Interest

The authors declare that they have no known competing financial interests or personal relationships that could have appeared to influence the work reported in this paper.

Acknowledgments

This work was supported by the Scientific Research Plan Projects of Shaanxi Education Department (18JK0780 and 12JK0532), the National Key Research and Development Program of China (2019YFC1520904), the Key Program for International Science and Technology Cooperation Projects of Shaanxi Province (2018KWZ-08), National Natural Science Foundation of China (61804125 and 61701402) and the start-up funds from Northwestern Polytechnical University (Grant 19SH020159 and 19SH020123). The authors of Vrije Universiteit Brussel (VUB) through the SRP-project M3D2 and the ETRO-IOF project.

REFERENCES

[1] Houska J. Maximum achievable N content in atom-by-atom growth of amorphous Si–C–N. ACS Appl Mater Interfaces 2020:8.
[2] Tomastik J, Ctvrtlik R, Ingr T, Manak J, Opletalova A. Effect of nitrogen doping and temperature on mechanical durability of silicon carbide thin films. Sci Rep 2018;8:1–17. https://doi.org/10.1038/s41598-018-28704-3.
[3] Zhang C, Qu L, Yuan W. Effects of Si/C ratio on the phase composition of Si-C-N powders synthesized by carbonitriding. Materials 2020;13:346. https://doi.org/10.3390/ma13020346.
[4] Katamune Y, Mori H, Morishita F, Izumi A. Control of the chemical composition of silicon carbon nitride films formed from hexamethyldisilazane in H_2/NH_3 mixed gas atmospheres by hot-wire chemical vapor deposition. Thin Solid Films 2020;695. https://doi.org/10.1016/j.tsf.2019.137750.
[5] Kozak AO, Porada OK, Ivashchenko VI, Ivashchenko LA, Scrynskyy PL, Tomila TV, et al. Comparative investigation of Si-C-N Films prepared by plasma enhanced chemical vapour deposition and magnetron sputtering. Appl Surf Sci 2017;425:646–53. https://doi.org/10.1016/j.apsusc.2017.06.332.
[6] Swain BP, Swain BS, Hwang NM. A comparative chemical network study of HWCVD deposited amorphous silicon and carbon based alloys thin films. J Alloys Compd 2014;588:343–7. https://doi.org/10.1016/j.jallcom.2013.11.105.
[7] Wrobel AM, Uznanski P, Walkiewicz-Pietrzykowska A, Jankowski K. Amorphous silicon carbonitride thin-film coatings produced by remote nitrogen microwave plasma chemical vapour deposition using organosilicon precursor. Appl Organomet Chem 2017;31:1–12. https://doi.org/10.1002/aoc.3871.
[8] Li Q, Yin X, Feng L. Dielectric properties of Si_3N_4-SiCN composite ceramics in X-band. Ceram Int 2012;38:6015–20. https://doi.org/10.1016/j.ceramint.2012.03.045.
[9] Chen Z, Lin H, Zhou J, Ma Z, Xie E. IR studies of SiCN films deposited by RF sputtering method. J Alloys Compd 2009;487:531–6. https://doi.org/10.1016/j.jallcom.2009.08.009.
[10] Li Q, Chen C, Xu M, Wang Y, Wang X, Zhang Z, et al. Blue-violet emission of silicon carbonitride thin films prepared by sputtering and annealing treatment. Appl Surf Sci 2021:149121. https://doi.org/10.1016/j.apsusc.2021.149121.
[11] Vassallo E, Cremona A, Ghezzi F, Dellera F, Laguardia L, Ambrosone G, et al. Structural and optical properties of amorphous hydrogenated silicon carbonitride films produced by PECVD. Appl Surf Sci 2006;252:7993–8000. https://doi.org/10.1016/j.apsusc.2005.10.017.

[12] Peng Y, Zhou J, Zhao B, Tan X, Zhang Z. Effect of annealing temperature and composition on photoluminescence properties of magnetron sputtered SiCN films. Thin Solid Films 2011;519:2083–6. https://doi.org/10.1016/j.tsf.2010.10.058.
[13] Du X, Fu Y, Sun J, Yao P. The evolution of microstructure and photoluminescence of SiCN films with annealing temperature. J Appl Phys 2006;99:093503. https://doi.org/10.1063/1.2194208.
[14] Xiao X, Li Y, Song L, Peng X, Hu X. Structural analysis and microstructural observation of SiC_xN_y films prepared by reactive sputtering of SiC in N_2 and Ar. Appl Surf Sci 2000;156:155–60. https://doi.org/10.1016/S0169-4332(99)00493-6.
[15] Ermakova E, Rumyantsev Y, Shugurov A, Panin A, Kosinova M. PECVD synthesis, optical and mechanical properties of silicon carbon nitride films. Appl Surf Sci 2015;339:102–8. https://doi.org/10.1016/j.apsusc.2015.02.155.
[16] Zhuang C, Schlemper C, Fuchs R, Zhang L, Huang N, Vogel M, et al. Mechanical behavior related to various bonding states in amorphous Si–C–N hard films. Surf Coating Technol 2014;258:353–8. https://doi.org/10.1016/j.surfcoat.2014.09.002.
[17] Tarntair FG, Wu JJ, Chen KH, Wen CY, Chen LC, Cheng HC. Field emission properties of two-layer structured SiCN films. Surf Coating Technol 2001;137:152–7. https://doi.org/10.1016/S0257-8972(00)01072-0.
[18] Swain BP, Hwang NM. Study of structural and electronic environments of hydrogenated amorphous silicon carbonitride (a-SiCN:H) films deposited by hot wire chemical vapor deposition. Appl Surf Sci 2008;254:5319–22. https://doi.org/10.1016/j.apsusc.2008.02.077.